Vertical dissipation profiles and the photosphere location in thin and slim accretion disks

Aleksander Sądowski[1], Marek A. Abramowicz[2,1],
Michal Bursa[3], Wlodek Kluźniak[4,1], and Agata Różańska[1]

[1] N. Copernicus Astronomical Center, Polish Academy of Sciences, Bartycka 18, 00-716 Warszawa, Poland
e-mail: `as@camk.edu.pl` e-mail: `wlodek@camk.edu.pl` e-mail: `agata@camk.edu.pl`
[2] Department of Physics, Göteborg University, SE-412-96 Göteborg, Sweden
e-mail: `Marek.Abramowicz@physics.gu.se`
[3] Astronomical Institute, Academy of Sciences of the Czech Republic, Bočni II/1401a, 141-31 Prague, Czech Republic
e-mail: `bursa@astro.cas.cz`
[4] Johannes Kepler Institute of Astronomy, Zielona Góra University, Lubuska 2, 65-265 Zielona Góra, Poland

ABSTRACT

As several authors in the past, we calculate optically thick but geometrically thin (and slim) accretion disk models and perform a ray-tracing of photons (in the Kerr geometry) to calculate the observed disk spectra. Previously, it was a common practice to ray-trace photons assuming that they are emitted from the Kerr geometry equatorial plane, $z = 0$. We show that the spectra calculated with this assumption differ from these calculated under the assumption that photons are emitted from the actual surface of the disc, $z = H(r)$. This implies that a knowledge of the location of the thin disks effective photosphere is relevant for calculating the spectra. In this paper we investigate, in terms of a simple toy model, a possible influence of the (unknown, and therefore ad hoc assumed) vertical dissipation profiles on the vertical structure of the disk and thus on the location of the effective photosphere, and on the observed spectra. For disks with moderate and high mass accretion rates ($\dot{m} > 0.01\dot{m}_C$) we find that the photosphere location in the inner, radiation pressure dominated, disk region (where most of the radiation comes from) does not depend on the dissipation profile and therefore emerging disk spectra are insensitive to the choice of the dissipation function. For lower accretion rates the photosphere location depends on the assumed vertical dissipation profile down to the disk inner edge, but the dependence is very weak and thus of minor importance. We conclude that the spectra of optically thick accretion disks around black holes should be calculated with the ray-tracing from the effective photosphere and that, fortunately, the choice of a particular vertical dissipation profile does not substantially influence the calculated spectrum.

Key words. accretion disks – vertical structure – photosphere

1. Introduction

There is a consensus that the observed spectra of black hole binaries and active galactic nuclei should be explained by accretion of rotating matter onto black holes. However, the available theoretical models of accretion disks do not provide a sufficiently detailed and accurate description of all physical processes that are relevant. There is neither a quantitative description of the turbulent dissipation that generates entropy and transports angular momentum, nor a fully self-consistent method to deal with the radiative transfer in the accreted matter.

Only partial solutions exist. Magnetohydrodynamic simulations provide useful information on the "radial" (Hawley & Krolik 2002) and "vertical" (Turner 2004) turbulent energy dissipation, but cannot yet simultaneously deal with the radiative transfer. On the other hand, all existing methods of solving the radiative transfer adopt some simplifying assumptions. Usually, they divide the flow into separate rings of gas and assume that each ring is in a hydrostatic equilibrium. They also assume ad hoc energy dissipation law (e.g. Davis et al. 2005; Różańska & Madej 2008; Idan et al. 2008). In most cases, radiative transfer with all important absorption and scattering processes treatment is implemented on the disc surface, while the deepest parts of the disk are treated in the diffusion approx-

imation. This simplification leads to a problem: the position of the disk photosphere is calculated only very roughly or is not calculated at all. In calculating the spectra, one usually assumes that all the emission takes place at the equatorial plane. However, in principle ray-tracing routines (e.g. Bursa 2006) should account for the precise location of the emission, especially for moderate and high accretion rates.

The spectrum computed "vertically" for each ring (i.e. at each radius separately), has to be integrated over the disk surface. This calls for a need of knowing the global "radial" structure of the accretion disk, consistent with the rings "vertical" structures adopted in the radiative transfer calculations. Expanding along these lines, we are working on constructing a new *vertical-plus-radial* code that inherits the sophisticated treatment of the radiative transfer from the works mentioned above, and at the same time fully incorporates our new radial, fully relativistic (in the Kerr geometry), transonic slim disk[1] code (described in Sądowski 2009).

---

[1] *Slim disk* is a transsonic solution of an optically thick accretion disk described by vertically integrated equations with simplified (limited to vertical force balance at the surface) treatment of its vertical structure (Abramowicz et al. 1988).
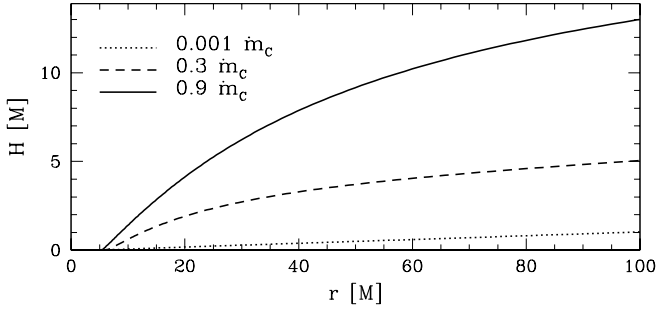
Fig. 1 Disk thickness obtained using slim disk model for non-rotating BH. Solutions for three mass accretion rates are presented: $\dot{m}$ = 0.001 (dotted line), 0.3 (dashed line) and $0.9\dot{m}_C$ (solid line). The critical mass accretion rate $\dot{m}_C$ corresponds to the Eddington luminosity of an accretion disk.

This paper addresses two questions concerning the effective photosphere of optically thick and geometrically thin or slim black hole (BH) accretion disk:

Is a knowledge of the exact photosphere location relevant for calculating the disk spectra?

Is the photosphere location sensitive to details of dissipative processes?

2. The calculated spectra depend on the location of the effective photosphere

We start with a simple demonstration that the calculated thin disk spectra depend on the location of the effective photosphere. For this purpose, we use the slim disk solutions that have been recently recalculated in the Kerr geometry by Sądowski (2009). We choose three particular models with the accretion rates,

$$0.001\dot{m}_C, \quad 0.3\dot{m}_C, \quad 0.9\dot{m}_C. \tag{1}$$

Here the critical accretion rate $\dot{m}_C$, defined as

$$\dot{m}_C = \frac{64\pi GM}{c\kappa_{es}} = 2.23 \times 10^{18}\frac{M}{M_\odot}\mathrm{g\cdot s^{-1}}, \tag{2}$$

corresponds to the Eddington luminosity of an accretion disk for a non-rotating BH.

Disk shapes, i.e. the functions $z = H(r)$ describing the vertical half-thickness, are presented in Fig. 1. For the lowest mass accretion rate ($0.001\dot{m}_C$) the H/r ratio for large radii is about 0.01 while for $\dot{m} = 0.9\dot{m}_C$ it reaches 0.13. Thus, for the accretion rates considered here, disks are always geometrically very thin,

$$H(r) \ll r. \tag{3}$$

(Note that for larger accretion rates, the slim disk thickness could be considerably higher.) The models calculated by Sądowski (2009) provide the local flux of radiation $F(r, \theta_e)$ in the frame of an observer comoving with the disk. In calculating the flux, the standard assumption have been adopted: (*i*) radiation from the effective photosphere is locally described by the black-body, (*ii*) the flux is limb-darkened by $F_{\mathrm{out}} \propto 2 + 3\cos\theta_e$, where θ_e is the emission angle relative to the effective photosphere normal vector. Using these initial fluxes, we ray-trace photons from the effective photosphere to an observer located 10kpc away from
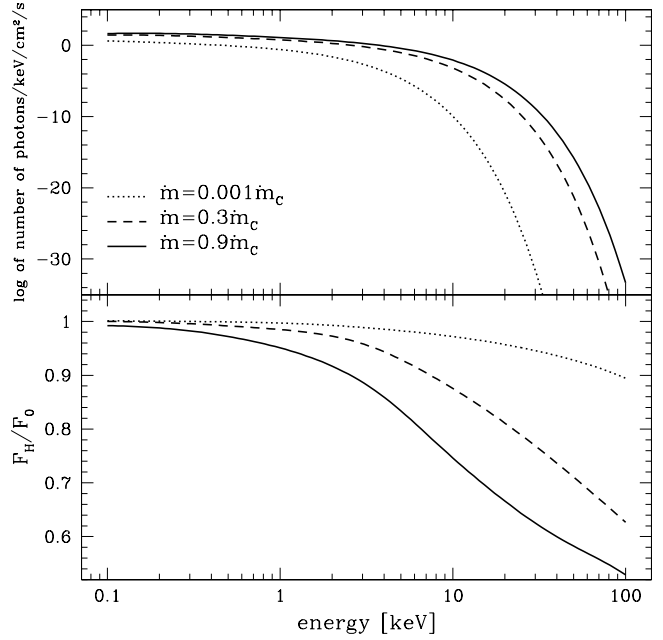

Fig. 2 Emerging spectra of accretion disks calculated using the slim disk model for three mass accretion rates and different assumptions about location of the emission for $M_{BH} = 9.4\,M_\odot$. The upper panel presents spectral fluxes calculated from the photosphere assuming distance to the observer $d = 10$kpc and the inclination angle $i = 60°$. The ratio of the photon flux obtained assuming photosphere emission to the photon flux obtained from the equatorial plane is plotted in the lower panel. For the spectral fitting purposes energy range $2 \div 20$keV is of the major importance.

the central black hole with mass $M_{BH} = 9.4\,M_\odot$ (the mass corresponds to the microquasar 4U 1543-17 while the order of magnitude of the distance can be considered typical for all BH binaries) and compute the observed spectra. We take into account all relativistic effects in the Kerr geometry (Bursa 2006).

For the three accretion rates (1), we calculate the disk spectrum twice: assuming that the effective photosphere coincides with the actual disk surface $z = H(r)$, or that it coincides with the equatorial plane $z = 0$, as if the disk would be infinitesimally thin. This means that in the first case we start ray-tracing from $z = H(r)$, and in the second case from $z = 0$.

The resulting spectra are plotted in Fig. 2. There are obvious differences between the spectra calculated with the two different assumptions about the location of the effective photosphere, i.e. the photosphere either at $z = H(r)$, or at $z = 0$. Even for the moderate mass accretion rate $0.3\dot{m}_C$, the "$z = 0$" spectral flux differs from the "$z = H(r)$" flux by about 20% at 20keV, and for higher accretion rates the difference is much higher. Such differences should certainly be considered as highly significant.

Thus, our result demonstrates that knowing the precise location of the effective photosphere is necessary in calculating the BH slim disk spectra. The effective photosphere lies certainly somewhere between the $z = H(r)$ and $z = 0$ surfaces. In principle, its location could strongly depend on details of the vertical dissipation, and this would be a rather bad news — these details are still not sufficiently well known and therefore ad hoc assumed in models.

In the rest of this paper we argue that such a situation is unlikely. Using a simple toy model for the vertical structure of geometrically thin, optically thick accretion disk, we show that the photosphere location is not highly sensitive to dissipation. Note, that for very thin (3) stationary disks the same is true for the total flux $F(r)$ emitted from a particular radial location — it does not depend on dissipation processes (Shakura & Sunyaev 1973).

These results strengthen one's confidence in estimating the black hole spin by fitting the observed spectra of black hole sources to these calculated theoretically (see e.g. Shafee et al. 2006; Middleton et al. 2006; Gou et al. 2009). However, they also indicate that the fitting procedures should be improved to include ray-tracing from the actual location of the photosphere.

3. A simple model of the vertical structure

Our simple model assumes that the accretion disk is geometrically thin (3) and that one may consider radial and vertical disk structure separately.

3.1. Radial equations

We do not solve radial equations, assuming instead that the rotation is strictly Keplerian (in the Kerr geometry),

$$\Omega = \Omega_K = \pm \frac{\sqrt{GM}}{r^{3/2} \pm a\sqrt{GM/c^2}} = \sqrt{\frac{GM}{r^3}}\frac{1}{\mathcal{B}} \tag{4}$$

and that the flux $F(r)$ follows from the mass, energy and angular momentum conservation (does not depend on radial dissipation) and is given by the standard formula (Novikov & Thorne 1973; Page & Thorne 1974),

$$F(r) = \frac{3}{8}\frac{GM\dot{M}}{\pi r^3}\frac{Q}{\mathcal{B}C^{1/2}}. \tag{5}$$

Herein M is the black hole mass, a is its specific angular momentum, and $\mathcal{A}(r,a)$, $\mathcal{B}(r,a)$, $C(r,a)$, $\mathcal{D}(r,a)$, $\mathcal{E}(r,a)$, $Q(r,a)$ are relativistic correction factors, defined as explicit functions of their arguments in Page & Thorne (1974).

3.2. Vertical equations

We describe the vertical structure of the BH accretion disk in optically thick regime by the following equations:

(i) The hydrostatic equilibrium:

$$\frac{\mathrm{d}P}{\mathrm{d}z} = -\rho\Omega_K^2\mathcal{G}z \tag{6}$$

where P is the sum of the gas and radiation pressures:

$$P = P_{gas} + P_{rad} = k\rho T + \frac{1}{3}aT^4 \tag{7}$$

and $\Omega_K^2\mathcal{G}z$ being the vertical component of the gravitational force of the central object calculated using the relativistic correction factor:

$$\mathcal{G} = \frac{\mathcal{B}^2\mathcal{D}\mathcal{E}}{\mathcal{A}^2C}. \tag{8}$$

(ii) The energy generation equation:

$$\frac{\mathrm{d}F}{\mathrm{d}z} = Q_{dis} \tag{9}$$

where F is the flux of energy generated inside the disk at a rate given by Q_{dis} - the dissipation rate which will be discussed in §5.1.

(iii) The generated flux of energy is transported outward through diffusion of radiation and/or convection according to the following thermodynamical relation:

$$\nabla = \frac{\mathrm{d}\ln T}{\mathrm{d}\ln P} \tag{10}$$

where ∇ is the thermodynamical gradient which can be either radiative or convective:

$$\nabla = \begin{cases} \nabla_{rad} & \text{dla } \nabla_{rad} \leq \nabla_{ad} \\ \nabla_{conv} & \text{dla } \nabla_{rad} > \nabla_{ad} \end{cases} \tag{11}$$

The radiative gradient ∇_{rad} is calculated using diffusive approximation:

$$\nabla_{rad} = \frac{3\kappa_R PF}{16\sigma T^4\Omega_K^2\mathcal{G}z} \tag{12}$$

where κ_R is the mean Rosseland opacity (see §3.3) and σ is the Stefan-Boltzmann radiation constant.

(iii) When the temperature gradient is steep enough to exceed the value of the adiabatic gradient ∇_{ad} we have to consider the convective energy flux. The convective gradient ∇_{conv} is calculated using the mixing length theory introduced by Paczyński (1969). Herein we take the following mixing length:

$$H_{ml} = 1.0H_P \tag{13}$$

with pressure scale height H_P defined as (Hameury et al. 1998):

$$H_P = \frac{P}{\rho\Omega_K^2 z + \sqrt{P\rho}\Omega_K} \tag{14}$$

The convective gradient is defined by the following formula:

$$\nabla_{conv} = \nabla_{conv} + (\nabla_{rad} - \nabla_{ad})y(y + V) \tag{15}$$

where y is the solution of the equation:

$$\frac{9}{4}\frac{\tau_{ml}^2}{3 + \tau_{ml}^2}y^3 + Vy^2 + V^2y - V = 0 \tag{16}$$

with the typical optical depth for convection $\tau_{ml} = \kappa_R\rho H_{ml}$ and V given by:

$$\frac{1}{V^2} = \left(\frac{3 + \tau_{ml}^2}{3\tau_{ml}}\right)^2 \frac{\Omega_K^2 z H_{ml}^2\rho^2 C_P^2}{512\sigma^2 T^6 H_P}\left(\frac{\partial\ln\rho}{\partial\ln T}\right)_P (\nabla_{rad} - \nabla_{ad}) \tag{17}$$

The thermodynamical quantities C_P, ∇_{ad} and $(\partial\ln\rho/\partial\ln T)_P$ are calculated using standard formulae (e.g. Chandrasekhar 1967) assuming solar abundances ($X = 0.70$, $Y = 0.28$) and taking into account, when necessary, the effect of partial ionization of gas on the gas mean molecular weight.

(iv) To close the set of equations describing the vertical structure of an accretion disk we have to provide boundary conditions. At the equatorial plane ($z = 0$) we put $F = 0$ while at the disk photosphere we require $F = \sigma T^4$ with the flux F given by Page & Thorne (1974).

3.3. Opacities

In this work we consider optically thick accretion disks. Therefore, we use Rosseland mean opacities κ_R. The opacities as a function of density and temperature are taken from Alexander et al. (1983) and Seaton et al. (1994). For temperatures and densities out of both domains we interpolate opacities between these two tables for intermediate values.

4. Numerical method

The set of ordinary differential equations defined in §3.2 is solved using Runge-Kutta method of the 4th order. We start integrating from the equatorial plane ($z = 0$) where we assume some arbitrary central temperature T_C, density ρ_C and set $F = 0$. We integrate given set of equations until we reach the photosphere which is defined as a layer where the following equation (corresponding to the optical depth $\tau = 2/3$):

$$\kappa_R P = \frac{2}{3} \Omega_K^2 \mathcal{G} z \tag{18}$$

is satisfied. If the temperature T and flux F does not satisfy the outer boundary condition ($F = \sigma T^4$) we tune up the value of the assumed central density ρ_C and again integrate starting from the equatorial plane. The converged solution is usually obtained after a few iteration steps. To get the photosphere profile $h(r)$ we look for the disk solutions at a number of radii in the range $r_{ms} < r \leq 200M$ with r_{ms} being the radius of the marginally stable orbit. At each radius we additionally search for the value of the central temperature which determines the solution with the emitted flux equal to the Novikov & Thorne value.

5. The photosphere location for a few ad hoc assumed vertical dissipation profiles

Herein we apply our simplified model of vertical structure (§3) to calculate photosphere location for different dissipation prescriptions. We test four families of dissipation functions described in the following section.

5.1. Dissipation profiles

First of all we apply the standard αP *prescription* given by Shakura & Sunyaev (1973). The authors assumed that the source of viscosity in accretion disk is connected with turbulence in gas-dynamical flow the nature of which was unknown at that time. They based on the following expression for the kinematic viscosity coefficient ν:

$$\nu \approx \nu_{turb} l_{turb} \tag{19}$$

(where ν_{turb} and l_{turb} stand for typical turbulent motion velocity and length scale, respectively). Shakura & Sunyaev assumed that the velocity of turbulent elements cannot exceed the speed of sound c_s as well as their typical size cannot be larger that the disk thickness h. Taking into account the expression for the $t_{r\phi}$ component of the viscous stress tensor in a Newtonian accretion disk:

$$t_{r\phi} = -\frac{3}{2} \rho \nu \Omega \tag{20}$$

and the standard form of the vertical equilibrium:

$$h \approx \left(\frac{P}{\rho}\right)^{1/2} \left(\frac{r^3}{GM}\right)^{1/2} \approx \frac{c_s}{\Omega} \tag{21}$$

one can limit the $t_{r\phi}$ in the following way:

$$-t_{r\phi} \leq \rho \Omega c_s h \approx \rho c_s^2 \approx P \tag{22}$$

Therefore, we may introduce a dimensionless viscosity parameter α satisfying the condition $\alpha \leq 1$:

$$t_{r\phi} = -\alpha P \tag{23}$$

This expression for viscosity is called *the α prescription* and has been widely and successfully used for many years in accretion disk theory. In this case the flux generation rate dF/dz (Eq. 9), given in the local rest frame by:

$$\frac{dF}{dz} = \sigma_{(r)(\phi)} t_{(r)(\phi)} = -\frac{3}{2} \frac{\mathcal{DB}}{C} t_{(r)(\phi)} \Omega_K \tag{24}$$

is expressed as:

$$Q_{dis} = \frac{dF}{dz} = \frac{3}{2} \frac{\mathcal{DB}}{C} \alpha P \Omega_K \tag{25}$$

In this work we apply the regular αP prescription for a few arbitrary values of the α parameter: $\alpha = 0.001, 0.01, 0.1, 0.2, 0.5, 1.0$.

In the last decade several authors (e.g. Sincell & Krolik 1998; Hubeny et al. 2001; Davis et al. 2005; Hui et al. 2005) used to apply a *constant dissipation rate* per unit mass. We follow them investigating a class of models using the following formula for the flux generation rate:

$$Q_{dis} = \frac{dF}{dz} = \frac{F_0}{m_0} \rho \tag{26}$$

Due to the fact that this expression requires not only the total emitted flux F_0 but also the total surface density m_0 one has to provide the latter basing on other disk solutions. In our work we use models calculated using regular α prescription for different values of α.

Recent numerical MHD simulations of stratified accretion disks in shearing box approximation (Davis et al. 2009) show that dissipation rate can be well approximated by the following formula:

$$Q_{dis} = \frac{dF}{dz} = \frac{1}{2} \frac{F_0}{\sqrt{m_0}} \frac{1}{\sqrt{m}} \rho \tag{27}$$

We apply it in another class of models ($m^{-1/2}$ *profile*). Similarly like in the *constant dissipation rate* case we impose surface density profile obtained using αP models.

Several authors investigated accretion disks with heat generation concentrated near the equatorial plane or close to the disk surface (e.g. Paczyński & Abramowicz 1982; Paczyński 1980). Therefore, we implement one more class of dissipation prescriptions with *arbitrary positioned* dissipation maximum. We use the following expression

$$Q_{dis} = \frac{dF}{dz} = \frac{dF}{dz}\bigg|_{\alpha P} e^{-\frac{(z-z_0)^2}{2d^2}} = \frac{3}{2} \frac{\mathcal{DB}}{C} \alpha P \Omega_K e^{-\frac{(z-z_0)^2}{2d^2}} \tag{28}$$

being flux generation rate for αP models re-scaled with Gaussian function centered at z_0 with dispersion parameter d given by:

$$z_0/r = d_{max} \qquad d/r = d_{disp} \tag{29}$$

where d_{max} and d_{disp} are constant for a given disk model.

In Fig. 3 we present dissipation profiles for a few exemplary models. The upper panel presents flux generation rate versus the vertical coordinate. The αP model (solid line) has bell-shaped dissipation profile where most of energy is generated at $z < 0.5H$. The model with constant dissipation rate per unit mass (thin dashed line) exhibits very similar behavior. The dissipation in no longer concentrated around the equatorial plane for the $m^{-1/2}$ model (thick dashed line) - the maximal flux generation is located at $z = 0.4H$. However, the dissipation profile is still extended through the whole disk thickness. The arbitrary positioned models (dot-dashed lines) show opposite behavior: the
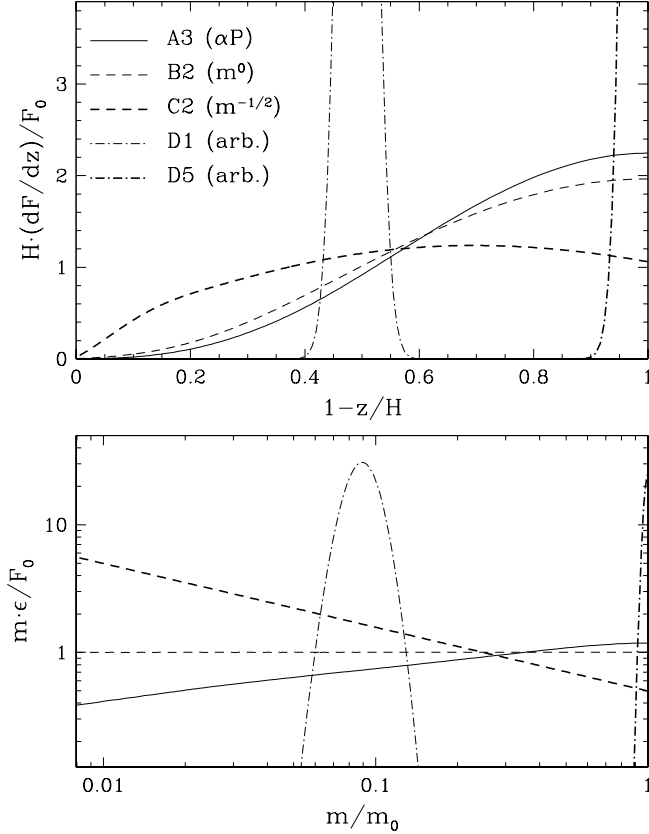
Fig. 3 Dissipation profiles for a few representative models at $r = 20M$. The upper panel presents dissipation functions versus the vertical coordinate z while the bottom panel versus surface density $m(z) = \int_H^z \rho(z)\,dz'$. On both panels left and right edges correspond to disk surface and equatorial plane, respectively. The models represent four families: aP (A3, solid line), constant dissipation rate per unit mass (B2, thin dashed line), $m^{-1/2}$ profile (C2, thick dashed line) and arbitrary positioned dissipation function (D1 and D5, dash-dotted lines).

energy generation is concentrated around an arbitrary given location. In case of the models presented in Fig. 3 the dissipation is confined to altitudes close to the equatorial plane ($z = 0$) and $z = 0.5H$.

Another point of view on the dissipation profiles is presented in the bottom panel of Fig. 3. The profiles are plotted against the fractional mass surface density m/m_0. The right edge of the figure ($m = m_0$) corresponds to the equatorial plane. Two families of models, with constant and proportional to $m^{-1/2}$ dissipation profiles, are represented by straight lines (they are power-law functions of m). As on the upper plot, one can notice similarity between the aP and constant dissipation rate models. The maximum of the flux generation rate for the arbitrary positioned model centered at $z = 0.5H$ corresponds to the mass depth $m = 0.1m_0$. Obviously, the model centered at the equatorial plane has maximal dissipation rate at $m = m_0$.

5.2. The photosphere location

We test a number of models representing all four classes of dissipation profiles for a moderate mass accretion rate $\dot{m} = 0.1\dot{m}_C$.

Details of model parameters are given in Tab. 1. The location of the disk photospheres is presented in Fig. 4. The first four panels present results for four classes of dissipation profiles in case of a non rotating BH. Common behaviour is clearly visible: all photosphere locations coincide at radii lower than $30M$. Outside this radius the location of the photosphere depends on the assumed dissipation profile and vary between $H/r \approx 0.03$ for the aP model with the highest value of $\alpha = 1.0$ and $H/r \approx 0.06$ for the lowest value $\alpha = 0.001$. It is of major importance to understand why all photosphere profiles coincide in the inner region which corresponds to the radiation pressure and electron scattering dominated regime of an accretion disk. The location of the photosphere is defined by Eq. 18. Wherever the radiation pressure and electron scattering dominate in a disk the left hand side of that formula depends only on the temperature which is connected at the photosphere with the outcoming flux by $F = \sigma T^4$. Therefore, the formula for the energy flux (Eq. 5) determines uniquely the location of the photosphere in the inner region of a disk *independently* of the assumed dissipation function. Under these assumptions we get from Eq. 18:

$$H = \frac{2F\kappa_{es}}{\Omega_K^2 \mathcal{G}c} \tag{30}$$

which describes perfectly the photosphere profiles presented in Fig. 4 for $r < 30M$.

Disk thickness profiles for a case of a rotating BH for three aP models are presented in the bottommost panel. They exhibit very similar behaviour: the photosphere location does not depend on the viscosity prescription for small radii corresponding to radiation pressure and electron scattering dominated region which, in case of a rotating BH with $a^* = 0.9$, extends inside $r = 40M$. Therefore, we may infer that such behaviour is general in accretion disks which exhibit radiation pressure dominated regimes. This statement is of paramount importance due to the fact that most of the emission from an accretion disk take place (in non-rotating case) between 6 and $20M$. As we have proven, for such radii the photosphere location should not depend on assumed dissipation profile and, therefore, the spectrum is likely to be independent of dissipation profile, either. However, one cannot make sure without performing full ray-tracing which would account for flux emitted from dissipation dependent regions correctly. Results of this procedure will be discussed in the following section. As Shakura & Sunyaev (1973) have shown for the lowest mass accretion rates the gas dominated region of an accretion disk may extend all the way down to the inner edge of a disk. For such case the behavior described in the previous paragraph is not expected: the photosphere profile should depend on the dissipation function at all radii. To account for this fact we compare photosphere profiles of accretion disks with low mass accretion rates (Fig. 5). For $\dot{m} = 0.1\dot{m}_C$ the radiation dominated region extends upto $r \approx 40M$. For lower accretion rate ($0.05\dot{m}_C$) it is confined to $r < 20M$, while for the lowest ($0.01\dot{m}_C$) it never appears. In that case the photosphere location indeed depends on the assumed viscosity prescription even for radii lower than $20M$ where most of the emission comes out. However, one has to bear in mind that H/r ratio for such low mass accretion rate is even below 0.015 and the impact of the photosphere location on the emerging spectrum should be insubstantial. It is studied in details in the following section.

5.3. Spectra

To assess the importance of different vertical dissipation profiles on emerging spectra we calculate them basing on photo-

Table 1 Model Assumptions for $\dot{m} = 0.1\dot{m}_C$

Model	Model family[a]	α	d_{max}	d_{disp}	a^*
A1	αP	0.001	-	-	0.0
A2	αP	0.01	-	-	0.0
A3	αP	0.1	-	-	0.0
A4	αP	0.2	-	-	0.0
A5	αP	0.5	-	-	0.0
A6	αP	1.0	-	-	0.0
AS1	αP	0.01	-	-	0.9
AS2	αP	0.1	-	-	0.9
AS3	αP	0.5	-	-	0.9
B1	constant diss. rate	0.01[b]	-	-	0.0
B2	constant diss. rate	0.1[b]	-	-	0.0
B3	constant diss. rate	0.5[b]	-	-	0.0
C1	$m^{-1/2}$	0.01[b]	-	-	0.0
C2	$m^{-1/2}$	0.1[b]	-	-	0.0
C3	$m^{-1/2}$	0.5[b]	-	-	0.0
D1	arbitrary positioned	0.1	0.0	0.001	0.0
D2	arbitrary positioned	0.1	0.02	0.001	0.0
D3	arbitrary positioned	1.0	0.0	0.001	0.0
D4	arbitrary positioned	1.0	0.02	0.001	0.0
D5	arbitrary positioned	1.0	0.02	0.0005	0.0
D6	arbitrary positioned	1.0	0.02	0.005	0.0

[a]Details of model assumptions are given in §5.1

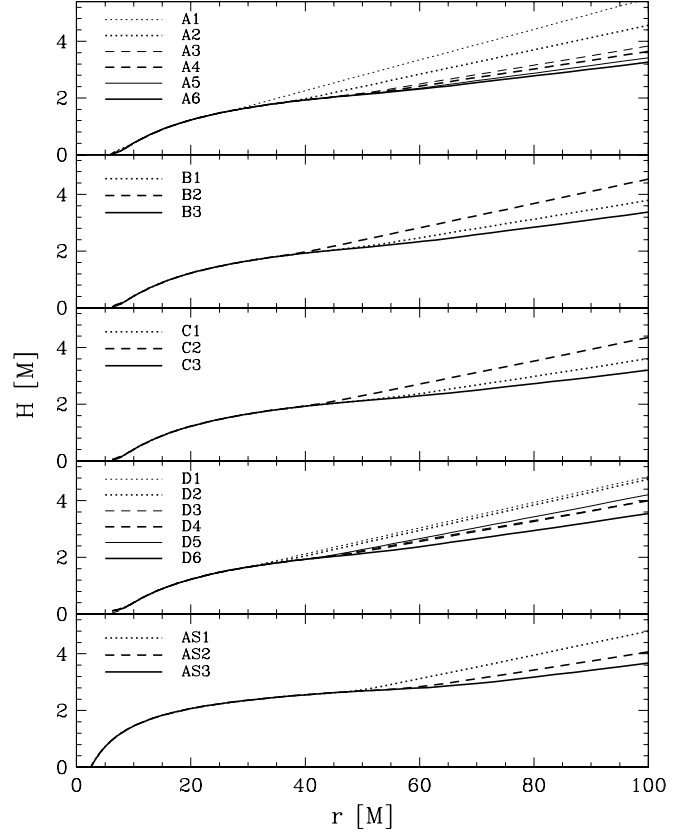[b]Calculated basing on surface density profiles obtained in the αP model with given α and a^*

Fig. 4 Photosphere profiles for different model families for $\dot{m} = 0.1\dot{m}_C$. The uppermost panel presents profiles for the αP models. The second one for models with constant dissipation rate per unit mass. The third one for $m^{-1/2}$ dissipation profile. The forth is for arbitrary positioned dissipation while the bottommost is for αP models in case of a rotating BH ($a^* = 0.9$). BH mass was 9.4 $M_\odot$. Model parameters are given in Table 1.

sphere profiles obtained using our model. For comparison, we also account for spectra calculated assuming emission from the equatorial plane. Spectra for models with mass accretion rate $\dot{m} = 0.1\dot{m}_C$ are presented in Fig. 6. The upper panel presents total spectra for non- and rapidly-rotating BH. The spectral profile for $a^* = 0.9$ case extends to higher energies due to the fact that accretion disk inner edge moves closer to the central object with increasing BH angular momentum extracting more energetic photons. Spectra for all the photosphere profiles almost coincide and differ significantly from spectra calculated assuming emission from the equatorial plane. It is clearly visible on the lower panel where we plot ratio of spectral fluxes emitted from the photosphere to emitted from the equatorial plane for two most extreme photosphere profiles (compare Fig. 4) for each value of BH angular momentum. The spectral profiles are identical up to a factor of 1%. The agreement is the best for energies of few keV. One may conclude that for accretion disks with sufficiently high accretion rate to form the inner radiation pressure supported region, the spectra depend only insignificantly on vertical dissipation profile in the most interesting range of energies (2.5 ÷ 20 keV; Gou et al. 2009). As was discussed in §5.2 for the lowest mass accretion rates ($< 0.05\dot{m}_C$) the inner, radiation pressure dominated disk region never appears and the photosphere location depends on the dissipation profile down to the disk inner edge. As it has been pointed out, such regime of accretion rates implies small values of the H/R ratio. To assess the impact of the dissipation profiles on the spectra we plotted ratios of corresponding spectral profiles for low and very low mass accretion rates (Fig. 7). The upper panel presents the ratios as observed by an observer perpendicular to the disk plane. The ratios approach 1 with decreasing mass accretion rate. The convergence is very slow due to the fact that disk thickness in disk outer region (gas pressure and free-free scaterings dominated) depends weakly on the mass accretion rate ($H \sim \dot{m}^{3/20}$,

Shakura & Sunyaev 1973). The difference in spectral fluxes between models with $\dot{m} = 0.1\dot{m}_C$ and $0.0001\dot{m}_C$ is no larger than 0.1% at 20keV. For inclined observer (the bottom panel) the departures from the equatorial plane model are much more significant (up to 10% at 20keV even for the lowest mass accretion rate). However, the difference between the spectral fluxes for the models with the two lowest mass accretion rates (corresponding to $H/R = 0.007$ and 0.015, respectively) is still of the order of 1% or even smaller. We conclude that in the lowest accretion rate regime changes of the photosphere location caused either by different mass accretion rates or different dissipation profiles are insignificant. However, one has to keep in mind that even for mass accretion rates as small as $0.0001\dot{m}_C$ taking into account the non-zero photosphere location is important for inclined observers as the spectral flux at high energies approaches the equatorial plane limit very slowly.

6. Discussion

Results presented here are very encouraging in the context of fitting the calculated optically thick spectra of slim accretion BH disk to the observed spectra. Our results imply that the major uncertainties of the accretion disk models, in particular the vertical
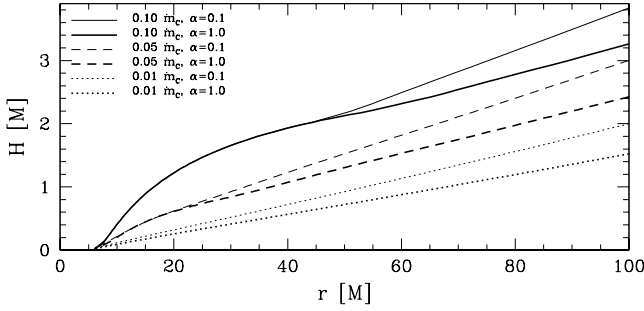
Fig. 5 Photosphere profiles for αP models for three different mass accretion rates ($\dot{m} = 0.10$, 0.05 and $0.01\dot{m}_C$) and two values of the α parameter (0.1 and 1.0). The regions where the photosphere profiles for a given accretion rate coincide are radiation pressure dominated. BH was non-rotating with $M = 9.4\,M_\odot$.
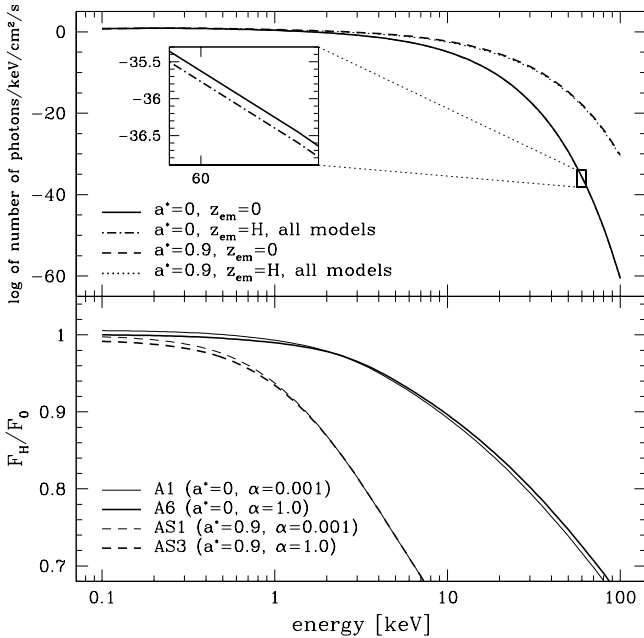

Fig. 6 Emerging spectra calculated for different models. The upper panel presents number of photons per energy crossing every second a unit surface assuming $d = 10\,\text{kpc}$. Spectra calculated assuming emission from the equatorial plane ($z_{em} = 0$) as well as from the photosphere surface ($z_{em} = H$) are presented for non-rotating ($a^* = 0$) and highly-spinning ($a^* = 0.9$) BH. The spectra for different dissipation profiles are indistinguishable - they all coincide with dot-dashed and dotted lines (depending on BH spin). The bottom panel presents ratio of the spectral flux (defined as above) calculated from the photosphere to the flux calculated from the equatorial plane for the models with extreme photosphere profiles (see §5.2). The inclination angle $i = 60°$.

dissipation profiles, have a rather small influence on the calculated spectra of steady disks with low accretion rates. This is a good news for these who use spectral fitting to estimate the black hole spin.

One should have in mind, however, that there are several effects that have been not taken into account in our simple model, and more theoretical work is needed before fully believable
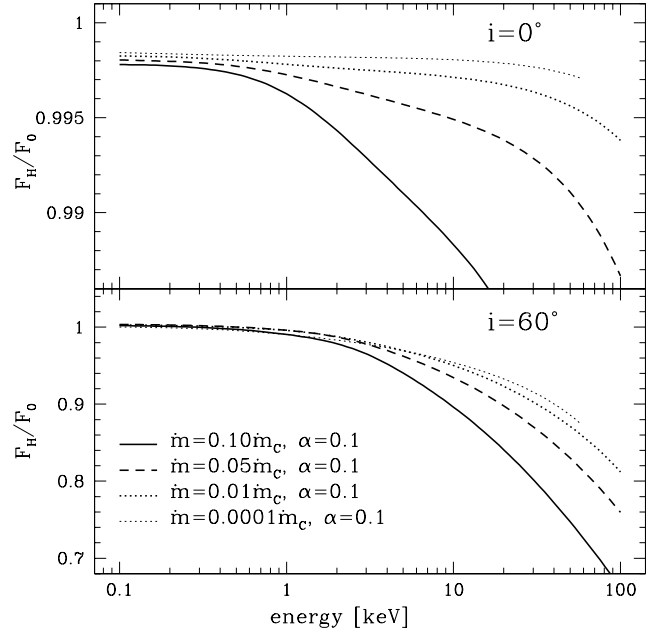

Fig. 7 Ratios of spectral profiles (photosphere to equatorial) for models with low mass accretion rates for the perpendicular ($i = 0°$, upper panel) and $i = 60°$ (lower panel) observers.

methods of calculating slim disk spectra will be at hand. One of the most obvious (and also quite challenging) theoretical developments needed is a self-consistent and simultaneous solving the vertical and radial structures of slim, optically thick black hole accretion disk. We are working on this problem.

References

Abramowicz, M. A., Czerny, B., Lasota, J. P., & Szuszkiewicz, E. 1988, ApJ, 332, 646
Alexander, D. R., Rypma, R. L., & Johnson, H. R. 1983, ApJ, 272, 773
Bursa, M. 2006, Ph.D. Thesis, Charles University, Prague
Chandrasekhar, S. 1967, An introduction to the study of stellar structure (New York: Dover, 1967)
Davis, S. W., Blaes, O., Hirose, S., & Krolik, J. H. 2009, ApJ, in preparation
Davis, S. W., Blaes, O., Hubeny, I., & Turner, N. J. 2005, ApJ, 621, 372
Gou, L., McClintock, J. E., Liu, J., et al. 2009, ArXiv e-prints
Hameury, J.-M., Menou, K., Dubus, G., Lasota, J.-P., & Hure, J.-M. 1998, MNRAS, 298, 1048
Hawley, J. F. & Krolik, J. H. 2002, ApJ, 566, 164
Hubeny, I., Blaes, O., Krolik, J. H., & Agol, E. 2001, ApJ, 559, 680
Hui, Y., Krolik, J. H., & Hubeny, I. 2005, ApJ, 625, 913
Idan, I., Lasota, J.-P., Hameury, J.-M., & Shaviv, G. 2008, ArXiv e-prints
Middleton, M., Done, C., Gierliński, M., & Davis, S. W. 2006, MNRAS, 373, 1004
Novikov, I. D. & Thorne, K. S. 1973, in Black Holes (Les Astres Occlus), 343–450
Paczyński, B. 1969, Acta Astronomica, 19, 1
Paczyński, B. 1980, Acta Astronomica, 30, 347
Paczyński, B. & Abramowicz, M. A. 1982, ApJ, 253, 897
Page, D. N. & Thorne, K. S. 1974, ApJ, 191, 499
Różańska, A. & Madej, J. 2008, MNRAS, 386, 1872
Seaton, M. J., Yan, Y., Mihalas, D., & Pradhan, A. K. 1994, MNRAS, 266, 805

Shafee, R., McClintock, J. E., Narayan, R., et al. 2006, ApJ, 636, L113
Shakura, N. I. & Sunyaev, R. A. 1973, A&A, 24, 337
Sincell, M. W. & Krolik, J. H. 1998, ApJ, 496, 737
Sądowski, A. 2009, ApJ, submitted
Turner, N. J. 2004, ApJ, 605, L45